Chen-Hu, K., Estrada-Jimenez, J. C., Garcia, M. J. F. G. & Armada, A. G. (2018). Continuous and Burst Pilot Sequences for Channel Estimation in FBMC-OQAM. *IEEE Transactions on Vehicular Technology*, 67(10), pp. 9711–9720.

DOI: 10.1109/tvt.2018.2861995

Continuous and Burst Pilot Sequences for Channel Estimation in FBMC-OQAM

Kun Chen-Hu, *Student Member, IEEE,*, Juan Carlos Estrada-Jiménez, *Student Member, IEEE,*, M. Julia Fernández-Getino García, *Member, IEEE,* and Ana García Armada, *Senior Member, IEEE.*

***Abstract*—Filter bank multi-carrier offset quadrature amplitude modulation (FBMC-OQAM) has advantages over the well-known orthogonal frequency division multiplexing (OFDM) due to its improved time-frequency efficiency. However, the self-interference of FBMC is an important issue in order to perform the channel estimation. To face this interference in FBMC, several pilot-based schemes have been proposed, but with a high complexity. We propose a novel approach, simple yet effective, based on the use of continuous pilot sequences (CPS) in FBMC. Our scheme considers an adequately designed pilot sequence, taking into account the self-interference, combined with a low-complexity channel estimation method which has a better performance in terms of mean squared error (MSE) and symbol error rate (SER) than previous methods proposed in the literature. Additionally, we also introduce burst pilot sequences (BPS), which have the same benefits of CPS while they reduce the number of required pilots and thus increase the available resources for data transmission. Moreover, we derive an analytical model to theoretically characterize the MSE of our proposed schemes. Simulation results have confirmed the validity of these theoretical expressions since their values perfectly match.**

***Index Terms*—pilot sequence, FBMC, channel estimation.**

I. Introduction

FILTER bank multi-carrier offset quadrature amplitude modulation (FBMC-OQAM) [1] [2] is considered as a waveform candidate in order to substitute the well-known orthogonal frequency division multiplexing (OFDM) [3]. FBMC-OQAM has a higher spectral efficiency, due to the suppression of the cyclic prefix (CP), and lower out-of-band emissions with the use of a well-designed prototype filter. Therefore, FBMC-OQAM can make a better use of the available spectrum, and allows to reduce the existing guard-bands.

Multi-carrier modulation systems require channel equalization in order to perform a coherent detection. In OFDM, several methods exist for this purpose. However, these existing methods cannot be straightforwardly used in FBMC-OQAM. The reason is the intrinsic self-interference caused by the surrounding symbols, due to the use of the prototype filters, that must be taken into account before the equalization process. Two alternatives for placing the pilot information for channel estimation in FBMC-OQAM are proposed in the literature, namely preamble-based [4] and scattered pilot-based [5] [6].

Focusing on scattered pilot-based techniques, the two classical ones are auxiliary pilot (AP) [5] and pair of pilots (POP) [6]. AP consists in transmitting an additional auxiliary pilot along with the traditional one. By doing so, the received pilots become interference-free, and channel estimation can be performed in the same way as in OFDM systems. However, this technique has two main drawbacks, one of them is that the minimum required power of the auxiliary pilot is about 3.3dB higher than the power of data symbols, which means an additional waste of the valuable energy and increasing the peak-to-average power ratio (PAPR); the second issue is the additional complexity added at the transmitter side which requires the computation of all the auxiliary pilots. POP transmits two precoded pilots which are capable of jointly compensating the self-interference. The receiver must perform a linear combination of the two received auxiliary pilots in order to get the estimated channel. However, due to this combination, it may increase also the noise which compromises the global performance.

Lately, several modifications based on the combination of AP and POP are proposed in order to solve the mentioned issues. Some of them are: precoded AP [7] [8], composite pilot pair (CPP) [9], dual-dependant pilots (DDP) [10] and interference-dependant pair of pilots (IDPOP) [11]. Precoded AP solves the power overhead of AP by precoding totally or partially the neighboring data. Unfortunately, this method is computationally complex and it only can be used when the density of pilots is extremely low. The rest of proposals consist in jointly computing two or three pilots in order to try, as far as possible, to avoid the power overhead at the transmitter side. Additionally, at the receiver side, they take advantage of the artificially enhanced self-interference of the pilots (known as pseudo-pilots) in order to improve the mean squared error (MSE) of the estimated channel. However, these improvements are made at the expense of increasing the complexity at both sides of the communication system. At the transmitter side, all the proposals are computing at least two pilots, instead of one as in AP. At the receiver side, CPP and IDPOP also require additional operations in order to get the channel estimation, similar to POP.

The additional complexity introduced by the mentioned techniques is not practical to be applied in some realistic communication systems. This is the case of machine type communications (MTC), where one of the constraints of user equipments (UE) is to enlarge the battery cycle as long as

The authors are with the Department of Signal Theory and Communications, Universidad Carlos III de Madrid (Spain). E-mail: {kchen, jestrada, mjulia, agarcia}@tsc.uc3m.es.

possible. Hence, the needed computations in order to deal with the self-interference could drain the battery of the UEs. Given this context, it is envisaged that novel strategies should be found to be able to estimate the channel in scattered pilot-based scenarios in FBMC-OQAM, but with an affordable complexity. Continuous pilot sequences (CPS) are widely used in many OFDM-based communication systems, such as: Digital Video Broadcasting Terrestrial (DVB-T) [12], or WiMax [13], among others. The main reason of using CPS is precisely when the channel is fast varying, because it provides its continuous tracking in order to improve the performance of the entire system. Additionally, besides the channel effects, there are other issues that should be taken into account as well, such as propagation attenuation, shadowing, antenna pattern, etc. [14]. CPS can be applied in the case of the recently proposed millimeter waves (mmWaves) [15] and in vehicular communications [16].

To the best of our knowledge, CPS has not been proposed before for FBMC-OQAM. Hence, the objective of this work is to propose an efficient combination of these two elements, which is not straightforward due to the presence of the self-interference in FBMC-OQAM, unlike in OFDM systems. At the transmitter side, the CPS must be specifically designed to work under this self-interference and avoid either any precoding procedures or enhancing the power overhead. At the receiver side, due to the adequate-design of CPS, a low-complexity averaging process is only required in order to reduce the noise and data interference, combined with the advantage of using pseudo-pilots in order to achieve a better channel estimation in terms of MSE. Hence, the low-complexity of CPS fits well with MTC, not only due to energy concerns, but also it makes low-cost devices even competitive in terms of price.

However, CPS is only advisable when the channel is quite unstable in order to provide a good tracking of it. On the contrary, when the variability of the channel is lower, CPS could be inefficient due to the considerable amount of allocated pilots in the system. Therefore, in order to face this inefficiency, we propose a variant of CPS denoted as burst pilot sequences (BPS). This scheme not only has the same benefits of CPS, but it also provides the flexibility to select the length of the pilot sequence depending on the variability of the channel in each moment, not only keeping the quality of the estimated channel, but also improving the number of available resources for data transmission. Moreover, we provide an analytical model to characterize the MSE of our proposed schemes that perfectly matches the simulation results. Finally, we compare our proposals to different schemes, available in the literature, in terms of computational complexity and symbol error rate (SER).

The remainder of the paper is organized as follows. Section II provides the system model of FBMC-OQAM. Section III proposes the novel CPS and BPS, specifically designed for FBMC-OQAM, and it describes the new channel estimation method. Section IV provides the analytical expression of the MSE. Section V shows the comparison of different schemes in terms of complexity. Section VI presents some numerical results to provide a better understanding of the performance of the entire system. Finally, in section VII some conclusions are pointed out.

Notation: $\mathbf{x}$ denotes a vector where $x[m]$ denotes its m-th element. $\mathbf{X}$ denotes a matrix where $X[m,n]$ denotes its element of the m-th row and n-th column. $\Re(x)$ and $\Im(x)$ are the real and imaginary part of x respectively. $*$ denotes the convolution operation. $\otimes$ denotes the Kronecker product of two matrices. $\mathbf{1}_{M,N}$ denotes a matrix of ones of size $M \times N$. $E[\mathbf{x}]$ denotes the expectation of $\mathbf{x}$. $E_N[\mathbf{x}] = (1/N)\sum_{n=0}^{N-1} x[n]$ denotes the average over N elements of $\mathbf{x}$. $diag\{\mathbf{x}\}$ denotes a diagonal matrix whose diagonal elements are $\mathbf{x}$. $tr\{\mathbf{X}\}$ denotes the sum of the diagonal elements of $\mathbf{X}$. $\sup(\mathcal{A})$ denotes the supremum of set $\mathcal{A}$. $\lceil x \rceil$ represents the smallest integer greater than or equal to x.

II. System Model

The system model is focused on a point-to-point link, where a FBMC-OQAM waveform is transmitted.

A. FBMC-OQAM

Let $\mathbf{S}$ denote a matrix containing the set of $M \times N/2$ complex data symbols to be transmitted, where M represents the number of parallel subcarriers and N is the number of time instants. The complex symbols belong to a K-QAM constellation with unit average power denoted as $\rho_s = 1$. Given $\mathbf{S}$, it is transformed into OQAM real symbols, where the real and imaginary parts of $\mathbf{S}$ are separated to build $\mathbf{S}_o$

$$S_o[m, n = 2n'] = \Re(S[m, n']), \tag{1}$$

$$S_o[m, n = 2n' + 1] = \Im(S[m, n']), \tag{2}$$

with $m = 0 \cdots M-1$ and $n' = 0 \cdots N/2 - 1$. Note that the size of $\mathbf{S}_o$ is $M \times N$, so n ranges here up to $N-1$. Additionally, the average power of $\mathbf{S}_o$ is $\rho_{so} = 0.5$.

The baseband model of the FBMC-OQAM transmitted signal is given by

$$x(t) = \sum_{n=0}^{N-1}\sum_{m=0}^{M-1} S_o[m,n] e^{j\phi[m,n]} g\left(t - n\frac{T_s}{2}\right) e^{j2m\pi f_s t}, \tag{3}$$

where $f_s = 1/T_s$ is the subcarrier spacing, T_s is the duration of the transmission of M samples, $g(t)$ is the real symmetric prototype filter impulse response and the phase $\phi[m,n]$ is given by

$$\phi[m,n] = \left\{ \begin{array}{ll} 0, & m+n \text{ even} \\ \frac{\pi}{2}, & m+n \text{ odd} \end{array} \right\}. \tag{4}$$

We define $g_{m,n}(t)$ as a time-frequency shifted version of $g(t)$, which can be expressed by

$$\begin{aligned} g_{m,n}(t) &= g\left(t - n\frac{T_s}{2}\right) e^{j2m\pi f_s t} e^{j\phi[m,n]} = \\ &= g_n(t)\, e^{j2m\pi f_s t} e^{j\phi[m,n]}. \end{aligned} \tag{5}$$

Therefore, we can rewrite (3) as

$$x(t) = \sum_{n=0}^{N-1}\sum_{m=0}^{M-1} S_o[m,n] g_{m,n}(t). \tag{6}$$

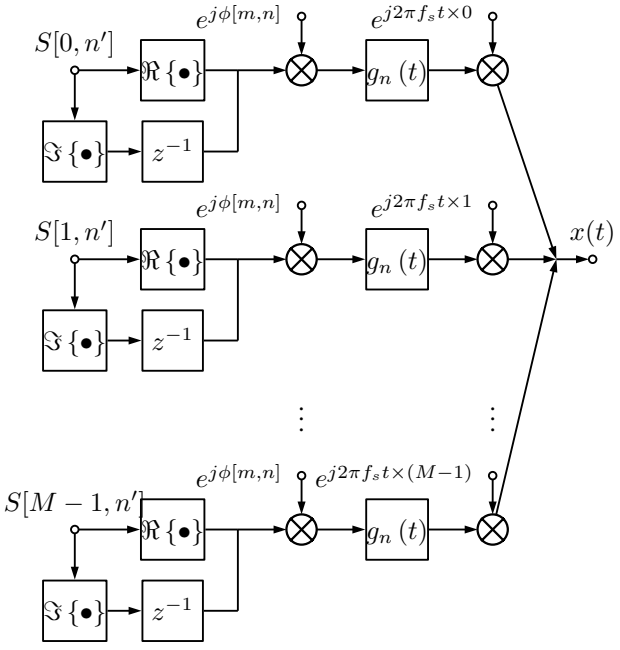

Fig. 1. Transmitter baseband model of FBMC-OQAM.

This operation is also known as the synthesis filter bank (SFB) (see Fig. 1). Note that $g(t)$ and $\phi[m,n]$ are designed so that $g_{m,n}(t)$ is orthogonal in the real field satisfying

$$\Re\{< g_{m,n}(t), g_{m',n'}(t) >\} = \left\{ \begin{array}{ll} 1, & m=m' \text{ and } n=n' \\ 0 & \text{otherwise} \end{array} \right\}. \tag{7}$$

In the absence of channel effects (distortion-free and noiseless) and assuming that we are sampling at the optimal point $n_0\frac{T_s}{2}$, the demodulated signal at subcarrier m_0 and symbol n_0 can be expressed by

$$\begin{aligned} R_o[m_0,n_0] &= \langle x(t), g_{m_0,n_0}(t)\rangle \Big|_{t=n_0\frac{T_s}{2}} = \\ &= \int_{-\infty}^{\infty} \left(\sum_n \sum_m S_o[m,n] g_{m,n}(t) g^*_{m_0,n_0}(t) \right) dt \Big|_{t=n_0\frac{T_s}{2}} = \\ &= \sum_n \sum_m S_o[m,n] \int_{-\infty}^{\infty} g_{m,n}(t) g^*_{m_0,n_0}(t) dt \Big|_{t=n_0\frac{T_s}{2}}. \end{aligned} \tag{8}$$

Applying (7), it is straightforward to show that the desired signal is always orthogonal to the self-interference, simplifying (8) in

$$\begin{aligned} &R_o[m_0,n_0] = \\ &= \underbrace{S_o[m_0,n_0]}_{\text{desired signal}} + \underbrace{\sum_{(m,n)\neq(m_0,n_0)} \sum S_o[m,n] v_{m_0,n_0}[m,n]}_{\text{self-interference}} \\ &= S_o[m_0,n_0] + jB[m_0,n_0], \end{aligned} \tag{9}$$

where $v_{m_0,n_0}[m,n] = \langle g_{m,n}(t), g_{m_0,n_0}(t)\rangle \Big|_{t=n_0\frac{T_s}{2}}$ is the coefficient which represents the interference caused in $[m_0,n_0]$ by each of the surrounding symbols placed at $[m,n]$, due to the joint effect of the residual components of the prototype filter $g(t)$ and additional phase rotation $\phi[m,n]$, and $B[m_0,n_0]$ denotes the whole self-interference amplitude at $[m_0,n_0]$. The operation in (8) is also known as the analysis filter bank (AFB) (see Fig. 2).

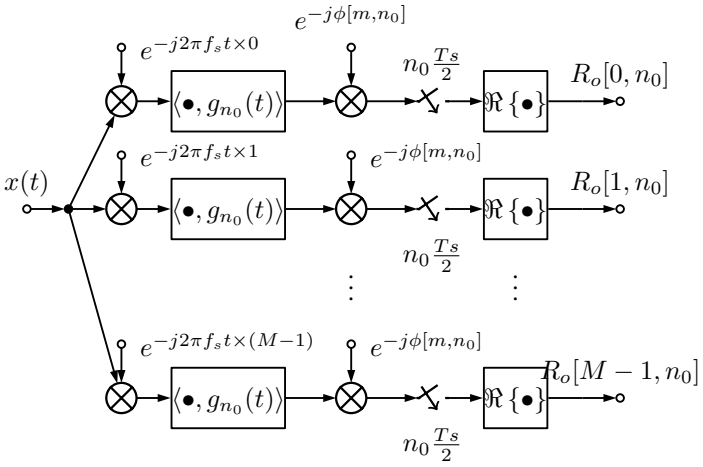

Fig. 2. Receiver baseband model of FBMC-OQAM.

Finally, all the original symbols $\mathbf{S}$ are recovered by

$$\begin{aligned} S[m_0,n_0'] =& \Re\left(R_o[m_0,n_0=2n_0']\right) + \\ &+ j\Re\left(R_o[m_0,n_0=2n_0'+1]\right). \end{aligned} \tag{10}$$

B. Effects of the channel in FBMC-OQAM

In the previous subsection, we have shown the analytical model for FBMC-OQAM under a scenario of absence of channel effects. However, in a realistic environment, the signal $x(t)$ goes through a frequency-selective fading channel. The received signal can be expressed as

$$y(t) = h(t,\tau) * x(t) + w(t), \tag{11}$$

where $h(t,\tau)$ represents the channel impulse response of the multipath channel with maximum delay spread τ_{max} and $w(t)$ is the additive white Gaussian noise (AWGN) with distribution $w \sim \mathcal{CN}(0,\sigma_w^2)$.

According to (11), (9) will be also modified by the channel effects. The received signal is given by

$$\begin{aligned} R_o[m_0,n_0] = H[m_0,n_0]\left(S_o[m_0,n_0] + jB[m_0,n_0]\right) + \\ + W[m_0,n_0], \end{aligned} \tag{12}$$

where $H[m_0,n_0]$ and $W[m_0,n_0]$ are the frequency response of the channel and noise respectively at subcarrier m_0 and symbol n_0. Note that $\mathbf{H}$ is a matrix of size $M\times N$, where each element is defined by

$$H[m,n] = H(f,t)\Big|_{f=mf_s,\quad t=n\frac{T_s}{2}}, \tag{13}$$

where $H(f,t)$ is defined in [17] by

$$H(f,t) = \int_0^{\tau_{max}} h(t,\tau) e^{-j2\pi f\tau} d\tau. \tag{14}$$

Additionally, $W[m_0,n_0]$ is the filtered noise, which is also a random variable with distribution $W \sim \mathcal{CN}(0,\sigma_w^2)$ defined in [2].

TABLE I
INTRINSIC INTERFERENCE CAUSED TO DATA PLACED AT $[m_0, n_0]$ USING THE PHYDYAS PROTOTYPE FILTER.

	n_0-3	n_0-2	n_0-1	n_0	n_0+1	n_0+2	n_0+3
m_0-1	$-j0.0429$	0.125	$j0.2058$	0.2393	$-j0.2058$	-0.125	$j0.0429$
m_0	-0.0668	0	0.5644	1	0.5644	0	-0.0668
m_0+1	$j0.0429$	-0.125	$-j0.2058$	0.2393	$j0.2058$	0.125	$-j0.0429$

III. CONTINUOUS AND BURST PILOT SEQUENCES FOR FBMC-OQAM

A. Continuous pilot sequences

Inspecting (12), we can see that FBMC-OQAM is using only half of the total amount of received power for transmitting data, since the other half is wasted by the self-interference term. In the particular case of channel estimation, the interference part must be taken into account in some way in order to get an accurate estimation, otherwise the performance of the entire system would be compromised.

We start analyzing how the interference is caused by the choice of the prototype filter in order to get some understanding of how to improve the channel estimation. To facilitate the analysis, we will use the PHYDYAS prototype filter [18], widely employed in the literature, as a particular case. In Table I, we can see the $v_{m_0,n_0}[m,n]$ coefficients when PHYDYAS prototype filter is used. We can clearly see that it is only well-localized in frequency since it only interferes two adjacent subcarriers. However, it is not localized in time, spreading the interference up to six contiguous symbols.

Let us define the vector $\mathbf{v}_m$ of size $(L_n \times 1)$, where $L_n = 6$, which represents the L_n black colored interference values of Table I, and vectors $\mathbf{v}_u$ and $\mathbf{v}_l$ of size $(L_v \times 1)$, where $L_v = 7$, which represent the L_v upper and lower gray colored interference values of Table I respectively. Note that the highest self-interference is caused by the symbol placed at $[m_0, n_0 - 1]$ and $[m_0, n_0 + 1]$. Additionally, their coefficients satisfy the following condition

$$tr\left\{diag\left\{\mathbf{v}_m\right\}\right\} \simeq 1. \tag{15}$$

Keeping these properties in mind, we can design continuous pilot sequences placed at every time instant, also known as pilot tones, which are capable of taking advantage of the self-interference over the time domain in order to enhance the power of the received pilot sequences (pseudo-pilots) and, hence, to improve the channel estimation. The idea of using pseudo-pilots is already considered by preamble-based techniques and IDPOP. By allowing the simultaneous transmission of pseudo-pilots with data symbols and through an adequate design of the pilot sequences, our proposal reduces the computational complexity at the receiver side, compared to IDPOP technique, while maintaining a good error performance as we will show.

According to (15), let us define a known pilot sequence vector $\mathbf{p}$, given by

$$\mathbf{p} = (p + jp)\,\mathbf{1}_{1,N/2}, \tag{16}$$

where $p = 1/\sqrt{2}$. Note that the proposed sequence has the same power as the data symbols, getting rid of the power overhead, unlike AP, and without any additional computation, unlike DDP. Applying (1) and (2) to (16), we obtain $\mathbf{p}_o$ which is defined by

$$\mathbf{p}_o = p\mathbf{1}_{1,N}. \tag{17}$$

To better analyze this problem, let us assume that we are sending a pilot sequence in any subcarrier m_0 (see Fig. 3a). Then in the absence of the channel effects, the received pseudo-pilot sequence $\mathbf{q}_o$ can be computed using (8) and (15), which is given by

$$q_o[m_0, n] = p[m_0, n] + jp[m_0, n]. \tag{18}$$

Observing (18), we can clearly see that the received pseudo-pilot not only has twice the power of the transmitted one (17) due to the self-interference, but also this interference term is a known value due to the property described in (15) combined with the well-designed pilot sequence (17). Additionally, note that $q_o[m_0, n]$ has the same value for any value of n, which facilitates the averaging process at the receiver side.

At the transmitter side, the M available subcarriers of $\mathbf{S}_o$ are split into two groups: one for data $\mathbf{S}_{o,d}$ of size $(M_d \times N)$ and another one for pilots $\mathbf{S}_{o,p}$ of size $(M_p \times N)$, where $M = M_d + M_p$. Although it may seem that CPS increments the pilot density, this is not so in the overall system. For the same pilot density in CPS as previous scattered pilot-based methods, CPS still outperforms those previous methods as we will show.

B. Burst pilot sequences

When the channel is not highly time-varying, the length of the pilot sequence (17) can be reduced in order to make a more efficient design, with the proposal of BPS (see Fig. 3b). The new pilot sequence $\mathbf{p}_o$ is defined by

$$\mathbf{p}_o = \begin{bmatrix} 0 & p\mathbf{1}_{1,N_b} & 0 \end{bmatrix}. \tag{19}$$

where $N_b + 2$ is the length of the burst sequence, and the two zeros at the beginning and at the end of the sequence are added in order to avoid the interference caused by the left and right data symbols that have the highest interference.

Given (19), it is obvious to see that the main advantage of BPS consists in that N_b can be designed according to the variability of the channel, so incrementing the data rate when the channel conditions allow it. The value of N_b can be characterized by the density of the sequence (ν), which is defined as

$$\nu = \frac{N_b + 2}{N_u} \leq 1, \tag{20}$$

where N_u is the total number of contiguous symbols in the time domain that will use the estimated channel obtained by the $N_b + 2$ pilots, where N_u includes the $N_b + 2$ pilots. Note that, the equality of (20) holds for CPS.

Additionally, N_u should satisfy that

$$N_u \leq \frac{T_c}{T_s/2}, \tag{21}$$

where T_c is the channel coherence time [19]. Otherwise, the performance of BPS is compromised.

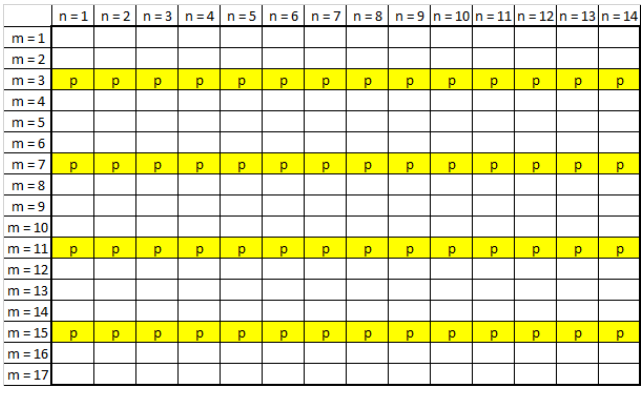

(a) CPS in FBMC-OQAM.

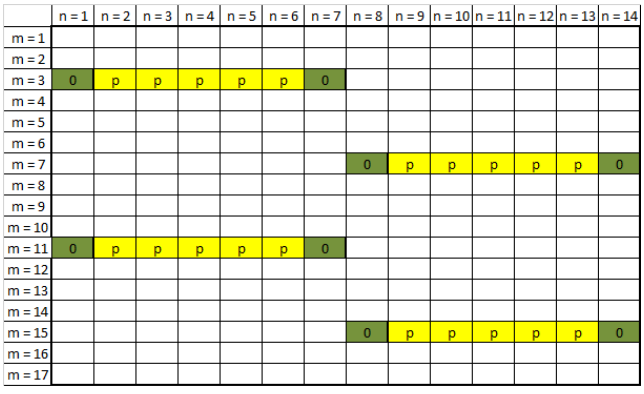

(b) BPS in FBMC-OQAM for $\nu = 0.5$.

Fig. 3. Layout of the pilot symbols in the time-frequency grid.

C. Channel Equalization for CPS and BPS

Given the system model detailed in the previous section, the received signal $\mathbf{R}_o$ can also be split into $\mathbf{R}_{o,d}$ and $\mathbf{R}_{o,p}$ which correspond to the received data and pilot sequences respectively. In general, any element of $\mathbf{R}_o$ can be expressed by (12). However, in the case of a received pilot sequence $\mathbf{R}_{o,p}$ can be decomposed by

$$\begin{aligned} R_{o,p}[m_0,n_0] &= H[m_0,n_0]\cdot \\ &\cdot \Big(p[m_0,n_0] + jp[m_0,n_0] + jC[m_0,n_0]\Big) + W[m_0,n_0], \end{aligned} \tag{22}$$

where $jC[m_0,n_0]$ is the interference caused by data symbols only placed at subcarriers m_0-1 and m_0+1 (see Table I), whose expression is given by

$$jC[m_0,n_0] = \sum_{n=n_0-3}^{n_0+3} \sum_{\substack{m=m_0-1 \\ m\neq m_0}}^{m_0+1} S_o[m,n] v_{m_0,n_0}[m,n]. \tag{23}$$

Comparing (9) and (23), it is obvious that $\rho_C < \rho_B$, where ρ_C and ρ_B correspond to the average power of $jC[m_0,n_0]$ and $jB[m_0,n_0]$ respectively, because the six interference terms from subcarrier m_0 are not included in the sum.

In order to estimate the channel, $\mathbf{R}_{o,p}$ is averaged over the variable n at m-th subcarrier, as follows

$$\begin{aligned} E_{N_g}\left[R_{o,p}[m,n]\right] = E_{N_g}\Big[H[m,n]\cdot\Big(p[m,n] + \\ + jp[m,n] + jC[m,n]\Big)\Big] + E_{N_g}\left[W[m,n]\right], \end{aligned} \tag{24}$$

where N_g is the number of averaged symbols. In the case of BPS, considering $N_g \leq N_b$, $N_g = N_b$ is a preferred choice, because a higher value of N_g corresponds to a lower interference due to the averaging process.

Without loss of generality, we focus in any N_g consecutive symbols out of N, $(n = n_0 \cdots n_0 + N_g - 1)$. Assuming that the channel frequency response is quasi-stationary in N_g symbols $(H[m,n] = h[m])$, and the pseudo-pilot sequence for the m-th subcarrier always contains the same value at every time instant, the expression (24) can be simplified as

$$\begin{aligned} E_{N_g}\left[R_{o,p}[m,n]\right] = h[m]\left(p[m] + jp[m]\right) + \\ + h[m]\underbrace{E_{N_g}\left[jC[m,n]\right]}_{C_{N_g}} + \underbrace{E_{N_g}\left[W[m,n]\right]}_{W_{N_g}}. \end{aligned} \tag{25}$$

Given the expression in (25), we can apply a Least Squares (LS) technique in order to estimate the channel using the pseudo-pilot $p + jp$, which is given by

$$\widehat{\mathbf{h}} = \left(E_{N_g}\left[\mathbf{R}_{o,p}\right]\right)\left(p + jp\right)^{-1}. \tag{26}$$

Once we have the estimated channel $\widehat{\mathbf{h}}$ for the pilot positions, we have to interpolate to obtain the values for the data indexes, according to

$$\widehat{\mathbf{h}}_{i[M_d\times 1]} = \mathbf{A}_{[M_d\times M_p]}\widehat{\mathbf{h}}_{[M_p\times 1]}, \tag{27}$$

where $\mathbf{A}$ is the matrix of interpolation coefficients.

Finally, in order to obtain the equalized symbols with a Zero-Forcing (ZF) technique, we just need to apply the following expression

$$\widehat{\mathbf{S}}_o = \left(\widehat{\mathbf{h}}_i \otimes \mathbf{1}_{1,N}\right)^{-1}\mathbf{R}_{o,d}. \tag{28}$$

IV. Analysis of Channel Estimation Error

The estimated channel differs from the original one due to not only the noise, but also the self-interference. Let us define the matrix $\widehat{\mathbf{H}}_p$ which contains M_p rows and, $\lceil N/N_g \rceil$ columns for CPS and $\lceil \nu N/\left(N_b+2\right) \rceil$ for BPS when considering $N_g = N_b$; and $\mathbf{H}_p$ corresponds to the actual channel coefficients of the same size. Therefore, the MSE can be defined and simplified by

$$MSE = E\left[\left|\widehat{\mathbf{H}}_p - \mathbf{H}_p\right|^2\right] = \sigma_H^2 E\left[\left|C_{N_g}\right|^2\right] + E\left[\left|W_{N_g}\right|^2\right], \tag{29}$$

where we have used the fact that $|p+jp|^2 = 1$ and $E\left[|H_p[m,n]|^2\right] = \sigma_H^2$. Using some Normal distribution properties [20], the probability density function (PDF) of W_{N_g} is given by

$$W_{N_g} \sim \mathcal{CN}\left(0, \frac{\sigma_w^2}{N_g}\right). \tag{30}$$

In order to characterize the term C_{N_g}, we will reformulate the total self-interference term. Let us compute the self-interference $\mathbf{c}_\phi$ at the m-th subcarrier for any N_g consecutive instants ($n = n_0 \cdots n_0 + N_g - 1$) as

$$\begin{aligned}\mathbf{c}_{\phi[N_g\times 1]} &= \mathbf{V}_{e[N_g\times 2L_T]}\mathbf{s}_{\phi[2L_T\times 1]} = \\ &= \begin{bmatrix}\mathbf{V}_{u[N_g\times L_T]} & \mathbf{V}_{l[N_g\times L_T]}\end{bmatrix}\mathbf{s}_\phi,\end{aligned} \tag{31}$$

where $L_T = L_v + N_g - 1$,

$$\mathbf{c}_\phi = \begin{bmatrix} C_\phi[m, n_0] \\ C_\phi[m, n_0+1] \\ \vdots \\ C_\phi[m, n_0+N_g-1]\end{bmatrix}, \tag{32}$$

$$\mathbf{s}_\phi = \begin{bmatrix} S_\phi[m-1, n_0-3] \\ \vdots \\ S_\phi[m-1, n_0+L_T-4] \\ S_\phi[m+1, n_0-3] \\ \vdots \\ S_\phi[m+1, n_0+L_T-4]\end{bmatrix}, \tag{33}$$

$$C_\phi[m,n] = C[m,n]e^{j\phi[m,n]}, S_\phi[m,n] = S_o[m,n]e^{j\phi[m,n]}, \tag{34}$$

$$\mathbf{V}_l = \begin{bmatrix} v_l[0] & \cdots & v_l[L_v-1] & 0 & \cdots & 0 \\ 0 & v_l[0] & \cdots & v_l[L_v-1] & \cdots & 0 \\ \vdots & \ddots & \ddots & \ddots & \ddots & \vdots \\ 0 & \cdots & 0 & v_l[0] & \cdots & v_l[L_v-1]\end{bmatrix}. \tag{35}$$

Note that $\mathbf{V}_u$ is built in the same way as $\mathbf{V}_l$ with $\mathbf{v}_u$ replacing $\mathbf{v}_l$, which are defined in Section III.

Given (31), we can rewrite C_{N_g} as

$$C_{N_g} = \frac{1}{N_g} tr\left\{diag\left\{\mathbf{c}_\phi\right\}\right\} = \frac{1}{N_g}\mathbf{v}_s^T\mathbf{s}_\phi, \tag{36}$$

where $\mathbf{v}_s$ is defined by

$$\mathbf{v}_{s[2L_T\times 1]} = \mathbf{V}_e^T\mathbf{1}_{N_g\times 1}. \tag{37}$$

In (36), C_{N_g} is a sum of $2L_T$ independent non-identically distributed discrete uniform random variables, whose PDF can be approximated by a Normal distribution using the central limit theorem (CLT) [21], so that

$$C_{N_g} \sim \mathcal{CN}\left(0, \frac{\rho_{so}\mathbf{v}_s^H\mathbf{v}_s}{N_g^2}\right). \tag{38}$$

Hence, if we use the Gaussian approximation, (29) can be simplified by

$$MSE = \frac{\rho_{so}\mathbf{v}_s^H\mathbf{v}_s}{N_g^2}\sigma_H^2 + \frac{M\sigma_w^2}{N_g}. \tag{39}$$

However, in a realistic scenario, L_T is not only a finite number, but also it is probably small, which may make the approximation inaccurate. In order to verify the accuracy of the approximation, we use the Berry-Essen theorem [22] that gives an upper-bound of the maximal error of approximation between the cumulative distribution function (CDF) of the normal distribution $\Phi(C_{N_g})$ and the true CDF distribution $F(C_{N_g})$ that we want to approximate, whose expression is given by

$$\varepsilon_{N_g} = \sup_{C_{N_g}\in\Re}\left|F(C_{N_g}) - \Phi(C_{N_g})\right| \leq 6\frac{\sum_{i=0}^{2L_T-1}\rho_i}{\left(\sum_{i=0}^{2L_T-1}\sigma_i^2\right)^{\frac{3}{2}}}, \tag{40}$$

where ρ_i and σ_i^2 are defined by

$$\rho_i = \left|\frac{\sqrt{\rho_{so}}v_s[i]}{N_g}\right|^3, \ \sigma_i^2 = \left(\frac{\sqrt{\rho_{so}}v_s[i]}{N_g}\right)^2. \tag{41}$$

The result of (40) is measured by the Kolmogorov-Smirnov distance [23], so we have to check if this measure satisfies the criteria of Kolmogorov-Smirnov test, which evaluates the similarity of two distributions. According to [23], the approximation is good enough when it satisfies

$$\begin{aligned}Pr\left(\sqrt{2L_T}\varepsilon_{N_g} \leq U_\alpha\right) &= \frac{\sqrt{2\pi}}{U_\alpha}\sum_{i=1}^{\infty}\exp\left(-\frac{\pi^2(2k-1)^2}{8i^2}\right) \\ &= 1-\alpha,\end{aligned} \tag{42}$$

where U_α is the confidence margin and α is typically 5%. Applying (42) to our case, it is straightforward to obtain that the result of the Gaussian approximation is accurate even for L_T as small as 7.

.

V. Computational Complexity

We evaluate the number of real operations required by our proposals, CPS and BPS, and other previously proposed schemes. Our references for the comparison are AP and DDP, because they are the schemes with the lowest number of required operations in the literature.

Without loss of generality, we only focus on one subcarrier of $\mathbf{S}_{o,p}$. In the case of AP [5] and DDP [10], their complexities depend on the number of pilots N_c placed during N symbols. On the contrary, CPS and BPS depend on N_g and N. Additionally, we also show the case of AP combined with the averaging of every two contiguous estimated channel values (AP2) in order to reduce the noise, which is a very common technique applied in OFDM [24]. In Table II, we show the evaluation of the complexity in terms of number of operations, before applying (26) [1].

Focusing on these schemes, DDP has twice the number of operations than AP and AP2. However, according to [10], DDP outperforms AP in terms of SER performance approximately by 2.5dB, which is almost the same improvement achieved by AP2 with half the number of operations.

Before comparing our proposed schemes with these ones, we should guarantee the same processing delay at the receiver side for all the schemes in order to make a fair comparison. This implies that $N_c = \lceil N/N_g \rceil$ (CPS) and $\lceil \nu N/\left(N_b+2\right)\rceil$ (BPS) and, in the case of AP and DDP, the estimated channel remains valid for N_g consecutive symbols. Moreover, we have also adopted this strategy for the simulations results. Under this assumption, it is clear that CPS and BPS require a much lower number of operations compared to the other schemes

[1] All methods require interpolation so it will add the same complexity.

proposed in the literature. Additionally, as we will see later in Section VI, CPS and BPS also outperform AP and AP2 for several values of N_g in terms of SER. These results make CPS and BPS an ideal candidate for low-consumption devices or delay-sensitive applications.

TABLE II
NUMBER OF REAL OPERATIONS PER SUBCARRIER.

	#real multiplications	#real adds
AP	$18 \times N_c$	$17 \times N_c$
AP2	$18.5 \times N_c$	$17.5 \times N_c$
DDP	$36 \times N_c$	$38 \times N_c$
CPS	$1 \times \lceil \frac{N}{N_g} \rceil$	$2(N_g - 1)$
BPS	$1 \times \lceil \nu \frac{N}{N_b+2} \rceil$	$2(N_b - 1)$

VI. NUMERICAL RESULTS

In this section we show some numerical results comparing the performance of AP, CPS and BPS schemes. We have discarded DDP due to the fact that it is a technique with the highest computational complexity, while it has a similar performance in terms of SER to AP2.

A. Simulation Parameters

In table III, we can see the numeric values for the parameters that we defined in the previous sections for CPS and BPS in FBMC-OQAM. We choose the well-known Long-Term Evolution (LTE) extended vehicular A (EVA) channel model [25] [26] for the power-delay profile. Additionally, we model time-variability with the Jakes Doppler spectrum [27], with 100Hz and 5KHz Doppler frequency. The coherence time [19] are 4.23 ms and 84.6 μs respectively. Also, the channel is normalized to $\sigma_H^2 = 1$.

TABLE III
SIMULATION PARAMETERS

M	64	**Overlap. Factor**	4
$\mathbf{M_d}$	48	**Prototype Filter**	PHYDYAS
$\mathbf{M_p}$	16	**Subc. Spacing**	15 KHz
Channel Model	LTE EVA	**Data Constellation**	QPSK
4 Slots $\rightarrow$ $\mathbf{N} = 4 \times 2 \times 7$ FBMC-OQAM symbols			

In the case of AP scheme, we are placing a total of $4 \times M_p$ pilot symbols ($2 \times M_p$ traditional and $2 \times M_p$ auxiliary pilots) for every slot, equally distributed over M subcarriers.

B. Definition of signal-to-noise ratio (SNR)

The SNR is defined by

$$\eta = E\left[|x(t)|^2\right] / \sigma_w^2. \tag{43}$$

Commonly, when comparing schemes with different spectral efficiency (e.g. due to the presence of CP in OFDM [28] or to coding [29]), the performance of the different channel estimation methods is evaluated by a comparison of the SER as a function of the E_S/N_0 ratio, where E_S is the useful symbol energy and N_0 the noise power spectral density. The computation of E_S/N_0 for the different proposals should take into account the energy wasted by the allocated pilot symbols, which means a reduction of the data efficiency. The expression is given by

$$\frac{E_S}{N_0} = \eta \frac{B_w}{R_S} \left(1 - \frac{M_p \times N_p}{M \times N}\right)^{-1}, \tag{44}$$

where R_S and B_w are the symbol rate and bandwidth respectively, and we assume that $R_S = B_w$; N_p is the number of pilots per subcarrier in one slot. In the case of AP $N_p = 16$, in CPS $N_p = N$, and in BPS is $N_p = \nu \times N$.

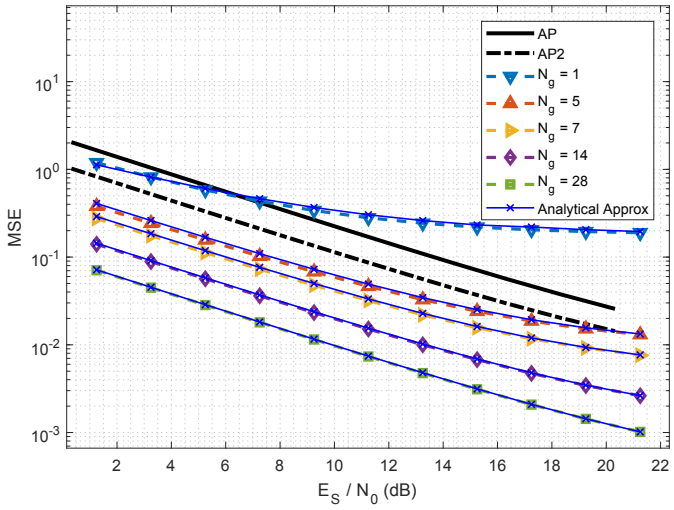

Fig. 4. MSE comparative of AP and CPS for different values of N_g and 7×10^3 channel realizations without any Doppler effects.

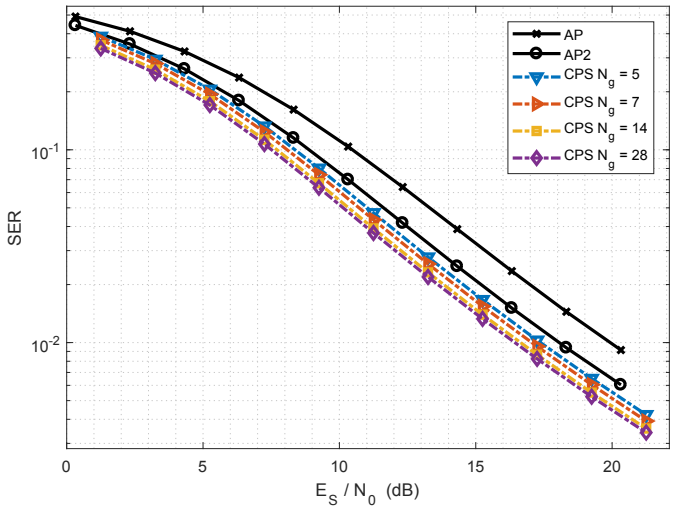

Fig. 5. SER comparative of AP and CPS for different values of N_g and 7×10^3 channel realizations without any Doppler effects.

C. Results

In Fig. 4, we present the comparative of the MSE, as defined in (29), for AP and CPS without considering Doppler effects. Moreover, in order to make a fair comparison, we also averaged two contiguous estimated channel values (AP2). It must be highlighted that results are plotted as a function of E_S/N_0, and thus, even though CPS and BPS may consider more pilot

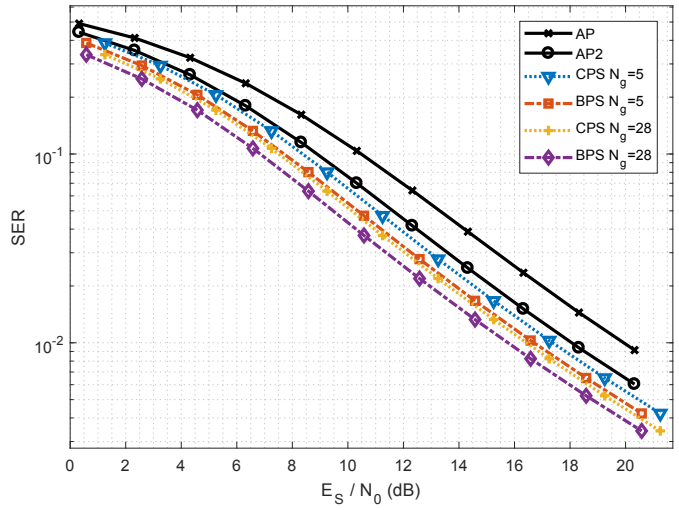

Fig. 6. SER comparative of AP, CPS and BPS with $\nu = 0.5$ and 7×10^3 channel realizations without any Doppler effects.

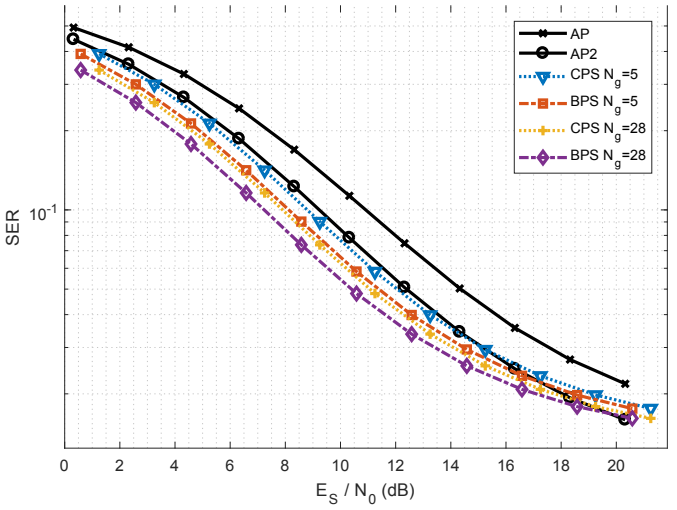

Fig. 8. SER comparative of AP, CPS and BPS with $\nu = 0.5$ in the presence of 100Hz Doppler frequency.

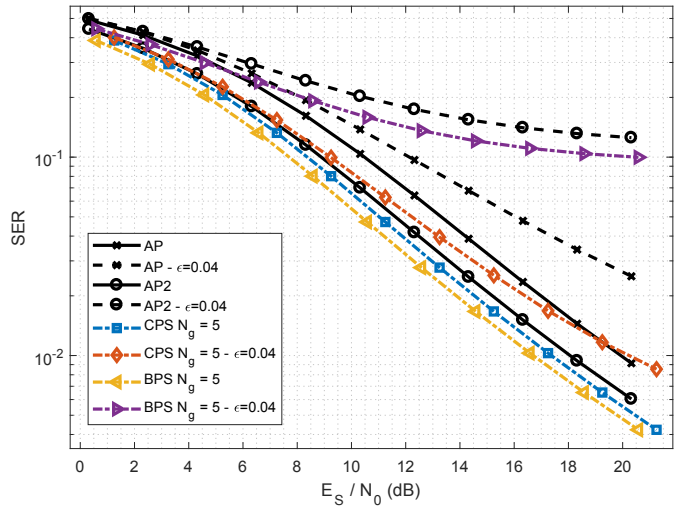

Fig. 7. SER comparative of AP, CPS and BPS under CFO effects with $\epsilon = 0.04, \nu = 0.5$ and 7×10^3 channel realizations without any Doppler effects.

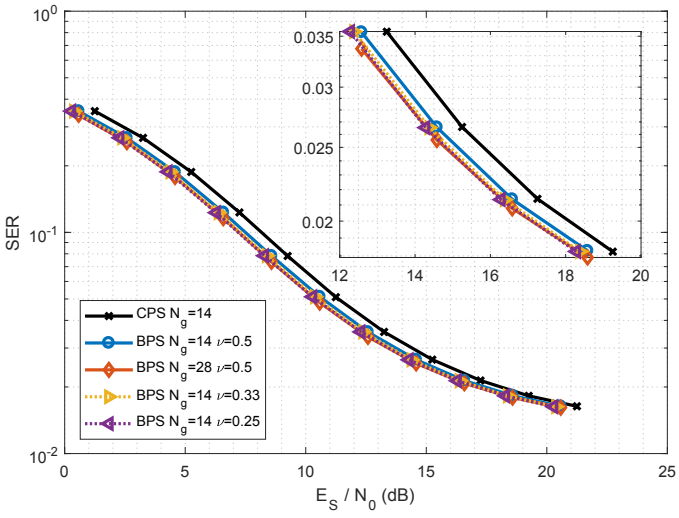

Fig. 9. SER comparative of CPS and BPS in the presence of 100Hz Doppler frequency.

symbols, this is accounted in (44) for a fair comparison. For all the considered values of N_g, CPS significantly outperforms AP and AP2. Moreover, we can see that our analytical Gaussian approximation is quite accurate even for $N_g = 1$, validating our theoretical analysis.

In Fig. 5, we show the comparative in terms of SER for AP and CPS without considering Doppler effects. We can see that CPS outperforms AP and AP2 for all the considered values of N_g. In the best case, CPS with $N_g = 28$ outperforms AP2 by 2dB. Note that the choice of $N_g = 28$ corresponds to 2 slots which is the minimum number of contiguous slots that are allocated to a given UE in LTE, making it a feasible value.

In Fig. 6, we provide the behavior of BPS, in terms of SER, compared to AP and CPS without considering Doppler effects. Theoretically, according to Section IV, if the channel remains quasi-stationary for N_u symbols and N_g is the same value for both schemes, the performance also must be the same for both techniques. However, BPS is more efficient than CPS in terms of pilot density ν, and therefore, the definition of E_S/N_0 (44) benefits BPS improving its performance by almost 1dB compared to CPS.

Additionally, in Fig. 7, we provide the same comparative that we have made in Fig. 6 with an additional effect of carrier frequency offset (CFO), where $\epsilon \in [0, 1]$ is the normalized residual CFO at the receiver, after a proper CFO estimation and compensation has been been performed. We can see that CFO adds an additional time variability to the system degrading the performance of all techniques. However, CPS provides the best SER thanks to its continuous tracking, and AP approaches are a worse solution than our proposals.

In Fig. 8, we illustrate the same comparative as in Fig. 6 with 100Hz Doppler frequency. In general, the performance suffers a significant degradation for every method compared to the case without any Doppler frequency. Nevertheless, the relative performance remains as in the previous cases. Analogously, our proposals CPS and BPS outperform AP and

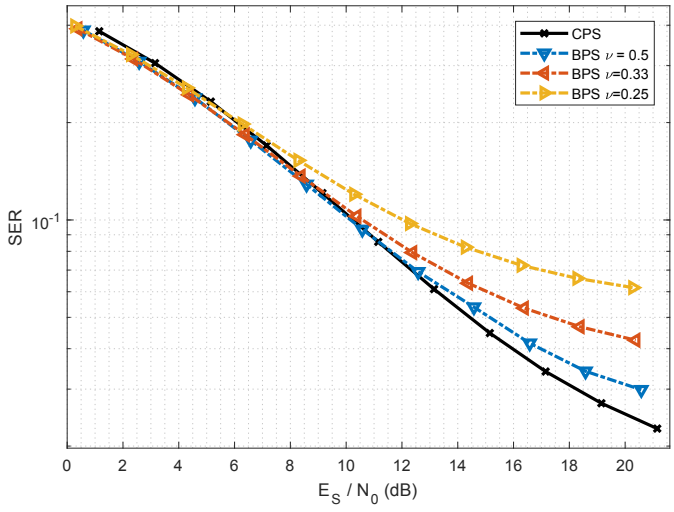

Fig. 10. SER comparative of CPS and BPS with $N_g = 14$ in the presence of 5KHz Doppler frequency.

also BPS provides better results than CPS, as stated before.

In Fig. 9, we present the performance of BPS for different values of ν with 100Hz Doppler frequency. We can see that BPS with $N_g = 14$ and $\nu = 0.25$ achieves the same result as BPS with $N_g = 28$ and $\nu = 0.5$. This means that we can not only increment N_g to improve the behavior, but also we can reduce the pilot density ν, which implies the increase of the efficiency in terms of data rate when the channel is slow-varying.

In Fig. 10, we show the comparative of CPS and BPS with 5KHz Doppler frequency which corresponds to a fast time-varying channel. We can clearly see that CPS has the same performance as BPS for low SNR, however when SNR is high, CPS outperforms all BPS variants. When the channel is very unstable, the continuous channel tracking performed in CPS is crucial, otherwise the performance of the system is compromised.

VII. Conclusions

In this paper we have proposed a combined technique based on the use of CPS or BPS with FBMC-OQAM. In this combination, we have introduced a specifically designed pilot sequence and an effective low-complexity technique to estimate the channel, which could be applied in any realistic communication system.

Numerical results show that the theoretical analysis using a Gaussian approximation is accurate to compute the channel estimation error. Additionally, they validate the behavior of our proposed system and its improvement compared to AP with its classical pilot scheme.

Acknowledgment

This work has been partly supported by Spanish National Projects ELISA (TEC2014-59255-C3-3-R), TERESA-ADA (TEC2017-90093-C3-2-R) (MINECO/AEI/FEDER, UE) and MACHINE (TSI-100102-2015-17); and also by National Secretary of Science, Technology and Innovation SENESCYT (Ecuador).

References

[1] S. Taheri, M. Ghoraishi, P. Xiao, and L. Zhang, "Efficient implementation of filter bank multicarrier systems using circular fast convolution," *IEEE Access*, vol. 5, pp. 2855–2869, Feb. 2017.

[2] L. Zhang, P. Xiao, A. Zafar, A. u. Quddus, and R. Tafazolli, "FBMC system: An insight into doubly dispersive channel impact," *IEEE Transactions on Vehicular Technology*, vol. 66, no. 5, pp. 3942–3956, May. 2017.

[3] T. Hwang, C. Yang, G. Wu, S. Li, and G. Y. Li, "OFDM and its wireless applications: A survey," *IEEE Transactions on Vehicular Technology*, vol. 58, no. 4, pp. 1673–1694, May. 2009.

[4] E. Kofidis and D. Katselis, "Improved interference approximation method for preamble-based channel estimation in FBMC/OQAM," in *2011 19th European Signal Processing Conference*, Aug. 2011, pp. 1603–1607.

[5] J. P. Javaudin, D. Lacroix, and A. Rouxel, "Pilot-aided channel estimation for OFDM/OQAM," in *the 57th IEEE Semiannual Vehicular Technology Conference, 2003. VTC 2003-Spring.*, vol. 3, Apr. 2003, pp. 1581–1585 vol.3.

[6] C. Lele, P. Siohan, R. Legouable, and J. P. Javaudin, "Preamble-based channel estimation techniques for ofdm/oqam over the powerline," in *2007 IEEE International Symposium on Power Line Communications and Its Applications*, Mar. 2007, pp. 59–64.

[7] C. Lele, R. Legouable, and P. Siohan, "Channel estimation with scattered pilots in OFDM/OQAM," in *2008 IEEE 9th Workshop on Signal Processing Advances in Wireless Communications*, Jul. 2008, pp. 286–290.

[8] W. Cui, D. Qu, T. Jiang, and B. Farhang-Boroujeny, "Coded auxiliary pilots for channel estimation in FBMC-OQAM systems," *IEEE Transactions on Vehicular Technology*, vol. 65, no. 5, pp. 2936–2946, May. 2016.

[9] Z. Zhao, N. Vucic, and M. Schellmann, "A simplified scattered pilot for FBMC/OQAM in highly frequency selective channels," in *2014 11th International Symposium on Wireless Communications Systems (ISWCS)*, Aug. 2014, pp. 819–823.

[10] B. Yu, S. Hu, P. Sun, S. Chai, C. Qian, and C. Sun, "Channel estimation using dual-dependent pilots in FBMC/OQAM systems," *IEEE Communications Letters*, vol. 20, no. 11, pp. 2157–2160, Nov. 2016.

[11] J. M. Choi, Y. Oh, H. Lee, and J. S. Seo, "Interference-dependent pair of pilots for channel estimation in FBMC systems," in *2016 IEEE International Symposium on Broadband Multimedia Systems and Broadcasting (BMSB)*, Jun. 2016, pp. 1–4.

[12] *Digital Video Broadcasting (DVB); Framing structure, channel coding and modulation for digital terrestrial television*, ETSI Std. ETSI EN 300 744, 2008.

[13] *IEEE Standard for Local and metropolitan area networks, Part 16: Air Interface for Broadband Wireless Access Systems*, IEEE Std. 802.16e, 2005.

[14] J. Xu, X. Yan, Y. Zhu, J. Wang, Y. Yang, X. Ge, G. Mao, and O. Tirkkonen, "Statistical analysis of path losses for sectorized wireless networks," *IEEE Transactions on Communications*, vol. 65, no. 4, pp. 1828–1838, April 2017.

[15] K. Guan, G. Li, T. Krner, A. F. Molisch, B. Peng, R. He, B. Hui, J. Kim, and Z. Zhong, "On millimeter wave and THz mobile radio channel for smart rail mobility," *IEEE Transactions on Vehicular Technology*, vol. 66, no. 7, pp. 5658–5674, Jul. 2017.

[16] X. Ge, H. Cheng, G. Mao, Y. Yang, and S. Tu, "Vehicular communications for 5G cooperative small-cell networks," *IEEE Transactions on Vehicular Technology*, vol. 65, no. 10, pp. 7882–7894, Oct. 2016.

[17] C. Lele, P. Siohan, R. Legouable, and J. P. Javaudin, "Preamble-based channel estimation techniques for OFDM/OQAM over the powerline," in *2007 IEEE International Symposium on Power Line Communications and Its Applications*, Mar. 2007, pp. 59–64.

[18] M. G. Bellanger, "Specification and design of a prototype filter for filter bank based multicarrier transmission," in *2001 IEEE International Conference on Acoustics, Speech, and Signal Processing. Proceedings (Cat. No.01CH37221)*, vol. 4, May. 2001, pp. 2417–2420 vol.4.

[19] T. S. Rappaport, *Wireless Communications: Principles and Practice, Second Edition*. Prentice Hall, 2002.

[20] B. Eisenberg and R. Sullivan, "Why is the sum of independent normal random variables normal?" *Mathematics Magazine*, vol. 81, no. 5, pp. 362–366, Dec. 2008.

[21] J. A. Rice, *Mathematical Statistics and Data Analysis.*, 3rd ed. Belmont, CA: Duxbury Press., 2006.

[22] W. Feller, *An Introduction to Probability Theory and Its Applications, Vol. 2*, 2nd ed. Wiley, 1971, vol. Volume 2.

[23] F. J. Massey, "The Kolmogorov-Smirnov Test for Goodness of Fit," *Journal of the American Statistical Association*, vol. 46, no. 253, pp. 68–78, 1951. [Online]. Available: http://www.jstor.org/stable/2280095
[24] Y.-S. Lee, H.-N. Kim, S. I. Park, and S. I. Lee, "Noise reduction for channel estimation based on pilot-block averaging in DVB-T receivers," *IEEE Transactions on Consumer Electronics*, vol. 52, no. 1, pp. 51–58, Feb. 2006.
[25] *User Equipment (UE) Radio Transmission and Reception*, 3GPP Std. 36.101, 2017.
[26] *Base Station (BS) radio transmission and reception*, 3GPP Std. 36.104, 2017.
[27] W. C. Jakes and D. C. Cox, Eds., *Microwave Mobile Communications*. Wiley-IEEE Press, 1994.
[28] A. Ikhlef and J. Louveaux, "An enhanced MMSE per subchannel equalizer for highly frequency selective channels for FBMC/OQAM systems," in *2009 IEEE 10th Workshop on Signal Processing Advances in Wireless Communications*, June 2009, pp. 186–190.
[29] V. M. Baeza, A. G. Armada, W. Zhang, M. El-Hajjar, and L. Hanzo, "A non-coherent multi-user large scale SIMO system relying on M-ary DPSK and BICM-ID," *IEEE Transactions on Vehicular Technology*, vol. PP, no. 99, pp. 1–1, 2017.

Kun Chen-Hu received his MSc degree in Multimedia and Communications in 2016 and MSc degree in Telecommunication Engineering in 2012, from Universidad Carlos III de Madrid (Spain). Currently, he is pursuing the Ph.D. degree at the same place and he belongs to the Communication Research Group. His research interests are signal processing, software-defined radio, waveforms design, massive MIMO systems and channel estimation.

Juan Carlos Estrada-Jiménez received B.E. degree from Escuela Politcnica Nacional (EPN), Quito, Ecuador, in 2009 and the M.Sc. degree in multimedia and communications from Carlos III University of Madrid (UC3M), Leganes, Spain in 2013. He joined the Communications Research Group, UC3M in 2015. He has been involved in ELISA and TERESA-ADA Projects. His research is focused in channel estimation strategies for new generation wireless communications.

M. Julia Fernández-Getino García (S99 - AM02 - M03) received the M. Eng. and Ph.D. degrees in telecommunication engineering from the Polytechnic University of Madrid, Spain, in 1996 and 2001, respectively. She is currently with the Department of Signal Theory and Communications, Carlos III University of Madrid, Spain, as an Associate Professor. From 1996 to 2001, she held a research position with the Department of Signals, Systems and Radiocommunications, Polytechnic University of Madrid. She visited Bell Laboratories, Murray Hill, NJ, USA, in 1998; visited Lund University, Sweden, during two periods in 1999 and 2000; visited Politecnico di Torino, Italy, in 2003 and 2004; and visited Aveiro University, Portugal, in 2009 and 2010. Her research interests include multicarrier communications, coding and signal processing for wireless systems.

She received the best "Master Thesis" and "Ph.D. Thesis" awards from the Professional Association of Telecommunication Engineers of Spain in 1998 and 2003, respectively; the "Student Paper Award" at the IEEE International Symposium on Personal, Indoor and Mobile Radio Communications (PIMRC) in 1999; the "Certificate of Appreciation" at the IEEE Vehicular Technology Conference (VTC) in 2000; the "Ph.D. Extraordinary Award" from the Polytechnic University of Madrid in 2004; the "Juan de la Cierva National Award" from AENA Foundation in 2004; and the "Excellence Award" from Carlos III University of Madrid in 2012 for her research career.

Ana García Armada (S96 - A98 - M00 - SM08) received the Ph.D. degree in electrical engineering from the Polytechnical University of Madrid in 1998. She is currently a Professor with the University Carlos III of Madrid, Spain, where she has occupied a variety of management positions (the Head of Signal Theory and Communications Department, the Vice-Dean of electrical engineering, a Deputy Vice-Chancellor of International Relations, among others). She is leading the Communications Research Group at this university. She has been a Visiting Scholar with Stanford University, Bell Labs, and the University of Southampton. She has participated in over 30 national and ten international research projects and 20 contracts with the industry, all of them related to wireless communications. She has co-authored eight book chapters on wireless communications and signal processing. She has authored around 150 papers in international journals and conference proceedings and she holds four patents. She has contributed to international standards organizations, such as ITU and ETSI. She is member of the expert group of the European 5G PPP. She has served on the TPC of more than 40 conferences and she has been/is part of the organizing committee of IEEE Globecom 2019, IEEE Vehicular Technology Conference (VTC) Fall 2018, IEEE Vehicular Technology Conference (VTC) Spring 2018 and IEEE 5G Summit 2017, among others. She is the Newsletter Editor of the IEEE ComSoc Signal Processing and Consumer Electronics Committee. She was the Secretary of the IEEE ComSoc Women in Communications Engineering Standing Committee and is now the Chair of this committee. She has served on the editorial boards of Physical Communication and the IET COMMUNICATIONS, and she serves on the editorial board of the IEEE COMMUNICATIONS LETTERS. She received the Young Researchers Excellence Award and the Award to Best Practices in Teaching, both from the University Carlos III of Madrid. She was awarded the third place Bell Labs Prize 2014 for shaping the future of information and communications technology. Her main interests are multicarrier and multi-antenna techniques and signal processing applied to wireless communications.